DOI: 10.38061/idunas.1727587

IDUNAS	NATURAL & APPLIED SCIENCES JOURNAL	2025 Vol. 8 No. 2 (1-12)

Investigation of the Laser Parameters that Should Be Used to Optimize the Root Mean Square Height Value, One of the Roughness Parameters Required to Obtain a More Hydrophobic Surface

Research Article

Timur Canel[1*], Çağla Pilavcı[2], Şeref Tosunoğlu[2,3]

[1] Kocaeli University, Faculty of Art and Sciences, Department of Physics, Kocaeli, Türkiye.
[2] Kocaeli University, Institute of Educational Sciences, Kocaeli, Türkiye.
[3] BS Petrol A.Ş., Kocaeli, Türkiye.

Author E-mails:
tcanel@kocaeli.edu.tr
cagla.pilavci@gmail.com
stosunoglu@hotmail.com
T. Canel ORCID ID: 0000-0002-4282-1806
Ç. Pilavcı ORCID ID: 0009-0005-5237-9598
Ş. Tosunoğlu ORCID ID: 0009-0004-2607-1584

*Correspondence to: Timur Canel, Kocaeli University, Faculty of Art and Sciences, Department of Physics, Kocaeli University, Kocaeli, Türkiye.

DOI: 10.38061/idunas.1727587

Received: 26.06.2025; Accepted: 17.10.2025

Abstract

This study investigates the effects of fiber laser surface texturing on ST52 steel plates to enhance hydrophobicity by optimizing surface roughness (Sq). Three key parameters—geometric pattern type (square, diamond, hexagon, circle), laser power (40–100 W), and theoretical laser-scanned area factor (20–80%)—were examined using a Taguchi L16 orthogonal array to minimize experimental runs while ensuring statistical validity. The goal was to maximize the Root Mean Square Height (Sq) for improved hydrophobic performance. The results revealed that the hexagonal pattern, 100 W laser power, and 80% scanning area produced the highest Sq value (338.39 µm), corresponding to a signal-to-noise (S/N) ratio of 50.59. ANOVA identified the scanning area factor (39.94%) as the most influential parameter, followed by laser power (34.29%) and pattern type (25.77%). Non-linear trends were observed: Sq peaked at 60 W and 100 W but dipped at 80 W, while the 80% scanning area yielded the roughest surface, and 40% the smoothest.

For hydrophobic applications, the optimal combination comprised circular or diamond patterns, an 80% scanning area, and laser powers of either 60 W or 100 W. Conversely, low-friction surfaces required square/hexagonal patterns, 40% scanning area, and 40 W or 80 W power. Overall, the

study demonstrates the efficacy of fiber laser texturing for tailoring ST52 steel surfaces and underscores the Taguchi method's utility in parameter optimization.

Keywords: Fiber laser texturing, ST52 steel, surface roughness (Sq), Taguchi method, hydrophobicity, laser power, geometric patterning.

1. INTRODUCTION

ST52 steel is a high-strength low-alloy (HSLA) structural steel characterized by its excellent mechanical properties, including high tensile strength, good weldability, and enhanced durability [1]. The designation "ST52" follows the German DIN standard (DIN 17100), where "St" stands for *Stahl* (steel) and "52" indicates a minimum yield strength of approximately 355 MPa [2]. This steel grade typically contains alloying elements such as manganese, silicon, and small amounts of carbon, which contribute to its enhanced load-bearing capacity and resistance to deformation under stress. Due to its favorable strength-to-weight ratio and adaptability to various fabrication processes—such as cutting, bending, and welding—ST52 steel is widely preferred in heavy-duty industrial and manufacturing applications. It is commonly used in the construction of bridges, cranes, and structural frameworks, where high mechanical strength is essential. Additionally, its robustness makes it suitable for machinery components, pressure vessels, and transportation equipment, including truck chassis and shipbuilding. The material's ability to withstand dynamic loads and harsh environmental conditions further solidifies its role in critical engineering applications, ensuring both structural integrity and long-term performance in demanding industrial settings [3].

Surface treatments modify the outermost layer of a material to achieve desired characteristics such as increased hardness, corrosion resistance, wear resistance, improved adhesion, or aesthetic appeal [4]. These modifications are critical in extending the service life of components, reducing maintenance costs, and ensuring reliability under harsh conditions. Common surface treatment methods include mechanical processes (e.g., shot peening, grinding), chemical treatments (e.g., anodizing, phosphating), electrochemical techniques (e.g., electroplating, electrophoretic deposition), and thermal processes (e.g., carburizing, nitriding) [5]. Additionally, advanced methods such as physical vapor deposition (PVD), chemical vapor deposition (CVD), and laser surface modification are employed for high-performance applications [6].

In the automotive industry, electroplating (e.g., chrome plating) is widely used for corrosion resistance and aesthetic finishes, while thermal spray coatings protect engine components from wear [7]. The aerospace sector relies on anodizing for aluminum components to prevent oxidation and on PVD coatings for turbine blades to withstand extreme temperatures [8]. In the medical field, passivation and electropolishing of stainless steel implants ensure biocompatibility and resistance to bodily fluids [9]. The construction industry often employs galvanizing (zinc coating) on steel structures to prevent rust [10], whereas the electronics industry uses thin-film deposition techniques to enhance conductivity and prevent oxidation in circuit boards [11]. By selecting appropriate surface treatments, industries optimize material performance, reduce failure rates, and comply with stringent operational and environmental standards.

Laser surface roughening is a precision surface engineering technique that employs focused laser beams to modify the topography of a material by creating controlled micro- or nanoscale roughness [12]. Unlike conventional mechanical or chemical roughening methods, this process is non-contact, localized, and highly controllable, allowing for selective texturing without inducing significant thermal distortion or material contamination. The laser's energy selectively ablates or melts the surface, forming patterns such as dimples, grooves, or hierarchical structures, depending on the laser parameters (e.g., wavelength, pulse duration,

power density, and scanning speed) [13]. This method is applicable to metals, polymers, ceramics, and composites, making it versatile for various industrial applications.

Laser surface roughening is preferred over traditional methods due to its precision, repeatability, and ability to enhance functional properties [14]**.** One of its key advantages is the improvement in surface adhesion, which is critical for coatings, bonding, and composite manufacturing. The controlled roughness increases the effective surface area, promoting mechanical interlocking and chemical bonding between substrates and coatings [15]. Additionally, laser roughening enhances tribological performance by optimizing lubrication retention in mechanical components, reducing friction and wear. In biomedical applications, such as orthopedic or dental implants, laser-textured surfaces improve osseointegration by encouraging cell adhesion and tissue growth. The process is also environmentally friendly, as it eliminates the need for hazardous chemicals used in acid etching or abrasive blasting. Furthermore, laser roughening can be automated and integrated into high-precision manufacturing systems, making it suitable for industries such as aerospace, automotive, electronics, and medical devices, where surface integrity and performance are critical.

The preference for laser surface roughening in industry stems from its adaptability and superior surface functionality. In the automotive and aerospace sectors, laser-textured surfaces on engine components, brake systems, and turbine blades enhance wear resistance and thermal management [16]. The electronics industry utilizes laser roughening to improve solderability and adhesion in printed circuit boards (PCBs) and semiconductor packaging [17]. In medical device manufacturing, titanium and polymer implants with laser-induced micro-textures exhibit better biocompatibility and reduced bacterial adhesion compared to smooth surfaces. Another significant advantage is the process flexibility—laser parameters can be fine-tuned to achieve specific roughness profiles (e.g., Ra, Rz) without altering bulk material properties [18]. Unlike mechanical abrasion, which may introduce subsurface damage, or chemical treatments, which can leave residues, laser roughening provides a clean and precise alternative. Moreover, advancements in ultrafast (femtosecond and picosecond) lasers have enabled nanoscale texturing, expanding applications in optics, microfluidics, and anti-reflective surfaces. Given these benefits, laser surface roughening is increasingly favored in high-tech industries where performance, durability, and precision are paramount.
The surface of ST52 steel is often intentionally roughened in industrial and manufacturing applications to enhance its functional performance in structural and mechanical components. As a high-strength low-alloy (HSLA) steel, ST52 is widely used in heavy-duty applications such as construction, shipbuilding, and machinery, where surface properties significantly influence durability, adhesion, and load-bearing efficiency. Roughening the surface improves mechanical interlocking for coatings, adhesives, and composite materials, ensuring stronger bonds and reducing delamination risks under stress. Additionally, a controlled rough surface can optimize lubrication retention in moving parts, reducing friction and wear in dynamic applications such as gears, bearings, and hydraulic systems. Unlike smooth surfaces, which may suffer from poor coating adhesion or premature failure due to cyclic loading, roughened ST52 steel exhibits improved fatigue resistance and long-term structural integrity.

Various surface roughening techniques are employed on ST52 steel, each selected based on cost, precision, and application requirements [19]. Mechanical methods such as grit blasting and grinding are commonly used for large-scale structures like bridges and ship hulls, where moderate roughness (Ra = 5–20 μm) is sufficient for paint or corrosion-resistant coatings. For more precise applications, such as automotive chassis components or industrial machinery, laser surface texturing (LST) is increasingly preferred due to its ability to create repeatable micro-patterns without introducing subsurface damage or thermal distortion. Chemical etching is another alternative, particularly in cases where electrochemical activation is needed before plating or bonding. The choice of methods depends on factors such as production scale, environmental considerations, and the need for post-treatment compatibility. For instance, in the manufacturing of pressure

vessels, a uniformly roughened surface ensures better adhesion of protective linings, preventing leaks and corrosion-induced failures. By enhancing surface characteristics, roughened ST52 steel meets stringent industrial demands for reliability, safety, and performance in harsh operating environments.

Surface roughness plays a critical role in determining the hydrophobic properties of a material, as it directly influences the interfacial interactions between a solid surface and a liquid droplet [20]. Hydrophobicity, characterized by a high-water contact angle (WCA > 90°), is governed by both surface chemistry and topography. According to the Wenzel and Cassie-Baxter models, roughness amplifies intrinsic wettability: a hydrophobic surface becomes more repellent when roughened, while a hydrophilic surface becomes more wettable. The Wenzel model suggests that roughness increases the actual surface area in contact with the liquid, enhancing existing wetting behavior. In contrast, the Cassie-Baxter model describes a composite state where air pockets are trapped between surface asperities, reducing liquid-solid contact and thereby increasing hydrophobicity. For highly rough surfaces, the Cassie-Baxter state often dominates, leading to superhydrophobicity (WCA > 150°), as seen in natural examples like lotus leaves and engineered surfaces such as microtextured polymers or laser-ablated metals [21].

The deliberate manipulation of surface roughness to achieve desired hydrophobic properties has significant applications across multiple industries [22]. In aerospace and automotive manufacturing, superhydrophobic coatings on aircraft wings or vehicle exteriors reduce ice adhesion and minimize drag, improving fuel efficiency. In marine engineering, roughened hydrophobic surfaces on ship hulls prevent biofouling and corrosion, extending service life. The medical field benefits from microtextured hydrophobic implants that resist bacterial adhesion and protein deposition. Advanced fabrication techniques, such as laser etching, electrochemical deposition, and nanoparticle coating, allow precise control over roughness parameters (e.g., Sa, Sz, Sq and skewness) to optimize hydrophobicity. However, excessive roughness can lead to mechanical fragility or inconsistent wettability, necessitating a balance between structural integrity and functional performance. Future research focuses on biomimetic designs and self-healing hydrophobic surfaces to enhance durability under extreme conditions. Understanding the roughness-hydrophobicity relationship thus enables the development of innovative materials for energy-efficient, anti-corrosive, and self-cleaning applications.

The Root Mean Square Height (Sq), a critical parameter in surface metrology, serves as a statistically robust measure of surface roughness by quantifying the standard deviation of height deviations from a mean plane [23,24]. Its relationship with hydrophobicity is rooted in the principle that Sq directly influences the interfacial contact area and energy between a liquid droplet and a solid surface, thereby modulating wettability behavior. According to the Wenzel and Cassie-Baxter wetting models, an increase in Sq amplifies the effects of intrinsic surface chemistry: for inherently hydrophobic surfaces (low surface energy), higher Sq values promote greater apparent contact angles by either enhancing surface area (Wenzel state) or facilitating air pocket entrapment (Cassie-Baxter state). Experimental studies on laser-textured metals and polymer composites demonstrate that superhydrophobicity (contact angle >150°) often correlates with Sq values in the micro- to nano-scale range (1–50 μm), where hierarchical roughness (combining high Sq with skewness/kurtosis control) optimizes liquid repellency. However, excessive Sq may destabilize the Cassie-Baxter state, causing wetting transitions to the Wenzel regime—highlighting the need for precise roughness optimization.

The predictive power of Sq in hydrophobicity is validated by interdisciplinary research linking quantitative roughness analysis to wetting dynamics. For instance, in nanostructured titanium dioxide coatings, an Sq threshold of ~20 nm was found critical to achieving stable superhydrophobicity, while larger Sq (~1–5 μm) in micropatterned polydimethylsiloxane (PDMS) surfaces enhanced durability against abrasion without compromising repellency. Notably, Sq alone is insufficient to fully describe hydrophobicity; synergistic

effects with other parameters (e.g., skewness (Ssk) for asymmetry or spatial density of peaks) are often necessary to account for air-trapping efficiency [25]. Advanced manufacturing techniques like ultrafast laser texturing and electrospinning allow precise Sq modulation, enabling tailored hydrophobic surfaces for applications such as anti-icing aircraft wings, microfluidic devices, and self-cleaning solar panels. Future research directions include machine learning models to correlate multi-scale roughness parameters (including Sq) with dynamic wetting behaviors, further refining the design of bioinspired hydrophobic materials.

In this study, the Root Mean Square Height (Sq), one of the surface roughness parameters required to achieve a more hydrophobic surface, was determined. Subsequently, the laser parameters necessary to obtain this value were optimized. The Taguchi optimization method and ANOVA tables were employed during the optimization process and in the analysis of the results. Finally, the effect of each laser parameter on the outcome was examined using mean effect plots.

2. MATERIAL AND METHODS

2.1 Optimization Method

Optimization techniques are essential in scientific and technical research because they make it easier to identify the best solutions to complex problems in a systematic and efficient manner [26]. Many engineering design processes—such as reducing system energy consumption, optimizing material use, or improving machine performance—involve making decisions based on multiple variables. Without optimization approaches, finding the ideal balance between competing objectives would require substantial time and resources.

In scientific research, optimization algorithms play a critical role in data processing, simulation, and model fitting. They enable researchers to adjust parameters and obtain accurate and reliable results. This is particularly valuable in fields such as computational biology, physics, and chemistry, where optimization supports experimental design and the solution of complex equations. Advanced optimization techniques—such as gradient-based algorithms, heuristic methods, and genetic algorithms—offer significant computational advantages, allowing researchers to address problems that would otherwise be unsolvable as datasets grow larger or as variable interactions become more complex. Consequently, optimization is indispensable for improving the efficiency and effectiveness of scientific and technical work, thereby fostering innovation and discovery.

Genichi Taguchi developed the Taguchi method as a statistical approach designed to improve process efficiency and product design by reducing variability and enhancing quality [27]. The Taguchi method is grounded in robust design principles and aims to minimize the sensitivity of processes or products to variations caused by uncontrollable external factors (noise), thereby increasing consistency and reliability. By employing orthogonal arrays to systematically design experiments, the method enables the simultaneous evaluation of multiple factors while significantly reducing the number of experiments required. This results in substantial savings in both time and cost while still providing valuable insights into the effects of multiple variables. Another important component of the Taguchi approach is the loss function, which quantifies the economic deviation from the desired performance and encourages both meeting design targets and minimizing variability.

The Taguchi method offers several advantages, including affordability, ease of implementation, and the ability to analyze multiple variables with minimal computational effort. It is particularly effective in

situations where conventional optimization methods are difficult to apply, such as when interactions between process variables are complex or when real-world experimentation is costly or impractical. The method is widely used in industrial sectors—especially electronics, automotive, and aerospace—to improve process efficiency and product quality. Applications include optimizing machining parameters, enhancing manufacturing processes, and developing high-performance materials. Beyond manufacturing, the Taguchi method has been applied in biotechnology, environmental engineering, and chemical processing, where minimizing variability and optimizing experimental conditions are crucial. Overall, the Taguchi method provides a systematic and efficient optimization framework applicable across diverse scientific and industrial domains.

Depending on the objective of a study, the Taguchi method employs three distinct quality characteristics. The "larger-the-better" characteristic is used when the goal is to maximize the response value, whereas the "smaller-the-better" characteristic is applied when the objective is to minimize the response. The "nominal-the-best" characteristic is selected when the target value is a specific numerical outcome. Three different calculation algorithms are used depending on these characteristics. These are:

$$S/_{N_i} = -10log_{10}\left[\frac{1}{n}\sum_{i=1}^{n}\frac{1}{y_{ij}^2}\right] \quad (1)$$

For Smaller the better characteristic.

$$S/_{N_i} = -10log_{10}\left[\frac{1}{n}\sum_{i=1}^{n}y_{ij}^2\right] \quad (2)$$

For Nominal the best characteristic.

$$S/_{N_{NB}} = -10log_{10}\left[\frac{1}{n}\sum_{i=1}^{n}(y_i - m)^2\right] \quad (3)$$

The goal of this research is to create the most stable hydrophobic surface possible. The adage "larger the better" was applied in this context.

2.2 Material and Experimental

In this study, the surfaces of 2 mm thick ST52 steel plates were machined using a high-precision fiber laser under various machining parameters listed in Table 1. Different geometric patterns were engraved onto the steel surfaces using fiber laser technology.

Four geometric designs—Square, Diamond, Hexagon, and Circle—were processed using four different laser power levels (40 W, 60 W, 80 W, and 100 W) and four different *theoretical laser scanned area factors* (80%, 60%, 40%, and 20%). The aim of the experiments was to investigate how surface energy, microstructural characteristics, and surface roughness change in response to variations in laser parameters and surface geometries. The textures were categorized according to the pattern type applied by the laser, and multiple experimental conditions were evaluated for each geometric design. The overall goal of the study is to examine the effects of laser processing parameters on ST52 steel surfaces and to determine the conditions required to achieve optimal surface properties.

Fiber laser systems, known for their reliability and efficiency, are capable of generating high-intensity laser beams and are widely used in marking, materials processing, and micromechanical applications. They are characterized by long operational lifetimes, high energy efficiency, low maintenance requirements, and superior beam quality. A fiber laser with a power output of 100 W is suitable for medium- to high-power applications and is effective for surface modification, marking, and metal cutting.
Three factors listed in Table 1 were examined at four different levels during the experiments. One of these parameters involves the classification of the surface pattern, while the remaining two are numerical processing parameters.

Table 1. Three machining parameters and their fours of levels.

Pattern Type	Scanned Area factor (%)	Laser Power (Watt)
Square	80	40
Diamond	60	60
Hexagonal	40	80
Circle	20	100

3. RESULTS AND DISCUSSION

When three components with four levels are examined, 34 (=81) experiments are needed according to traditional experimental design. Effective results can be obtained with fewer experiments when optimization techniques are used. In this study, the Taguchi method—which has demonstrated strong performance in many scientific and engineering fields—was used. According to the Taguchi technique, the first step is to select the appropriate orthogonal array to minimize the number of experiments. For this investigation, the L16 orthogonal array was chosen because it accommodates three parameters with four levels each. The L16 orthogonal array was used to organize the laser machining experiments listed in Table 1, and the experimental sets were constructed accordingly. The experimental configurations and averages of Root Mean Square Height values of the surfaces obtained with these configurations are listed in Table 2.

In this study, the primary objective is to achieve the highest S_q value (Root Mean Square Height across the Surface) to obtain a more hydrophobic surface. For this purpose, the "larger-is-better" characteristic provided in Equation 2 was adopted. The Root Mean Square Height (S_q) values obtained from the analysis of the topographies of all laser-processed surfaces, as well as the corresponding S/N ratios calculated from these values, are presented in Table 2.

Table 2. Root Mean Square Height (Sq) and Signal-to-Noise (S/N) Values Across the Surface for All Experiments

	Texture	**Scanned area factor (%)**	**Power (W)**	**S_q**	**S/N values of contact angle**
1	Square	80	40	55.20	34.84
2	Square	60	60	163.00	44.24
3	Square	40	80	23.00	27.23
4	Square	20	100	129.00	42.21

Table 2 (continuous)

5	Diamond	80	60	254.00	48.10
6	Diamond	60	40	49.40	33.87
7	Diamond	40	100	93.30	39.40
8	Diamond	20	80	221.00	46.89
9	Hexagon	80	80	290.00	49.25
10	Hexagon	60	100	160.00	44.08
11	Hexagon	40	40	197.00	45.89
12	Hexagon	20	60	46.60	33.37
13	Circle	80	100	225.00	47.04
14	Circle	60	80	192.00	45.67
15	Circle	40	60	45.30	33.12
16	Circle	20	40	28.80	29.19

Statistical reliability was tested by calculating the total sum of squares. The ANOVA results are shown in Table 3. The highest levels were obtained as follows: for pattern type, "3rd level - (Hexagonal)," for scanning area ratio, "1st level - (80 W)," and for laser power, "4th level - (100 W)." The expected S/N and S_q values for the optimum combination were calculated as "50.59" and "338.39," respectively.

Table 3. ANOVA table for Hydrophobicity (larger S_q) according to the Taguchi Method.

	Average S/N						
Factors	1. Level	2. Level	3. Level	4. Level	Factors	Optimum Level	Optimum Parameter
Pattern	37.13	42.06	43.15	38.75	25.77	3	Hexagonal
Scanned Area	44.81	41.97	37.51	37.91	39.94	1	80 %
Power	35.95	39.71	42.26	42.88	34.29	4	100 W
Average		40.27					
Total					100.00		
Optimum S/N							50.59
Optimum S_q							338.39

The most effective parameter for achieving a more hydrophobic surface was found to be the scanning area, with a contribution rate of 39.94%. The second most influential parameter was laser power, contributing 34.29%. Among the parameters examined, the least effective was the pattern type formed on the surfaces, with a contribution rate of 25.77%. The main effect plots for hydrophobicity are presented in Figure 1 (see Section 3.1).

3.1. Effects of Laser Processing Parameters on the Arithmetic Average Height (S_a) of a Surface

This section examines how laser processing parameters influence the Arithmetic Average Height (Sa) of the surface. The main effect plots are presented in Figure 1.

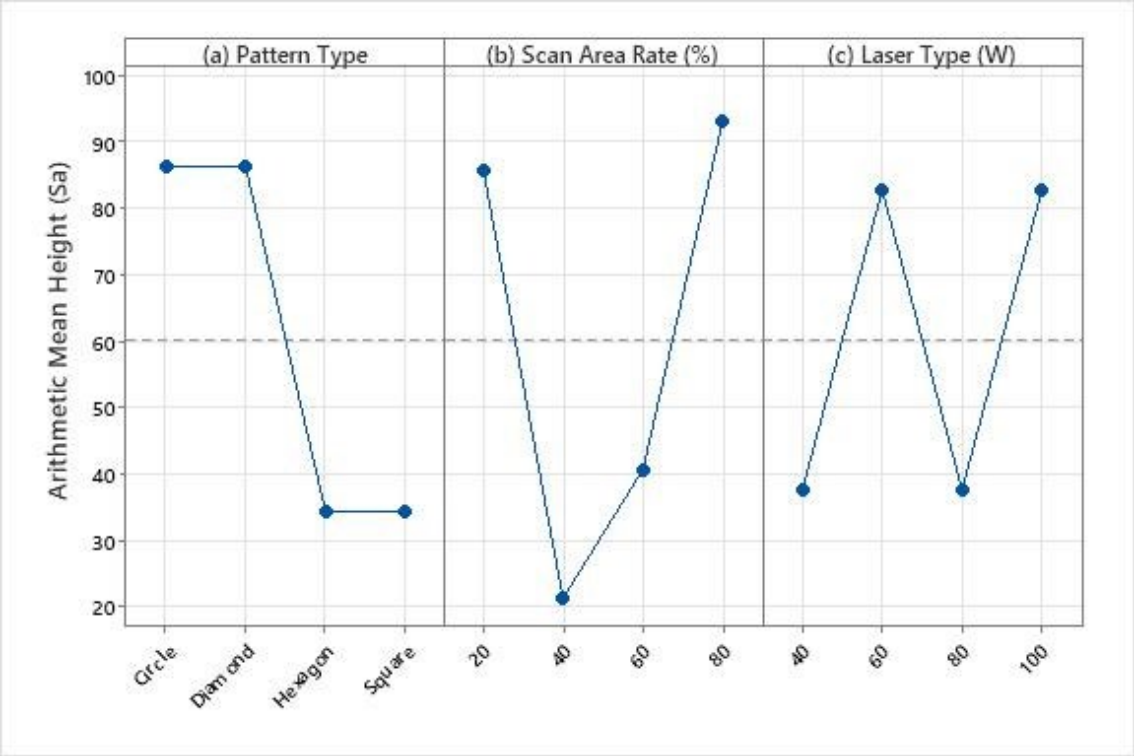

Figure 1. Main Effect Plots for the Effects of Laser Processing Parameters on the Arithmetic Average Height (S_a) of a Surface

As shown in Figure 1(a), the circular and diamond design types had the highest Sa values, whereas the hexagonal and square patterns yielded the lowest Sa values. The effect of scanning area on Sa is depicted in Figure 1(b), where an increase in scanning area from 20% to 40% resulted in a sharp drop in Sa. The Sa value then rapidly climbed to its maximum value as the scanning area was expanded from 40% to 60% and subsequently to 80%. The scanning region with the highest Sa value was 80%, and the one with the lowest Sa value was 40%.

Figure 1(c), which shows how laser power affects Sa, shows that the Sa value rose quickly as the laser power increased from 40 W to 60 W. Nevertheless, the Sa value dropped almost as quickly when the laser power was raised from 60 W to 80 W. The Sa value then rose at a comparable pace when the laser power was raised from 80 W to 100 W.

A higher Sa value is required to achieve a more hydrophobic surface. The main effect plot shows that the circular and diamond patterns produced the highest Sa values, indicating improved hydrophobicity due to increased surface roughness. In addition, the 80% scanning-area condition yielded the highest Sa values among all tested levels. Laser power also significantly affected roughness: the highest Sa values were obtained at 60 W and 100 W. Therefore, to produce a more hydrophobic surface, the optimal combination includes the circular or diamond pattern type, an 80% scanning area, and a laser power level of either 60 W or 100 W.

In contrast, a lower Sa value is desirable when the goal is to obtain a surface with a lower friction coefficient. The main effect plot shows that the hexagonal and square patterns produced the lowest Sa values, making them more suitable for applications requiring smoother surfaces. The lowest Sa value was observed at a 40% scanning area. Additionally, the 40 W and 80 W laser power levels generated relatively low Sa values

compared to the other levels. Consequently, the optimal condition for achieving reduced friction consists of the hexagonal or square pattern type, a 40% scanning area, and a laser power of either 40 W or 80 W. Overall, the results indicate that hydrophobicity and friction are controlled by different optimal parameter combinations. Surfaces requiring high hydrophobicity benefit from high roughness (high Sa), whereas applications requiring reduced friction benefit from lower roughness (low Sa). The circular/diamond patterns and higher scanning areas enhance roughness, while the hexagonal/square patterns and moderate scanning areas produce smoother surfaces..

4. CONCLUSION

This study investigated the influence of laser processing parameters—including geometric pattern type, laser power, and theoretical laser-scanned area factor—on the surface characteristics of ST52 steel plates, with a focus on achieving enhanced hydrophobicity through increased Root Mean Square Height (Sq). Utilizing the Taguchi method, an L16 orthogonal array was employed to optimize experimental efficiency while maintaining statistical reliability. The key findings and conclusions are summarized below:

1. Optimal Parameters for Hydrophobicity:

- The hexagonal pattern (3rd level) produced the highest Sq values, followed by circular and diamond patterns, indicating superior surface roughness conducive to hydrophobicity.
- A laser power of 100 W (4th level) and a scanning area ratio of 80% (1st level) were identified as optimal for maximizing Sq, with predicted S/N and Sq values of 50.59 and 338.39, respectively.

2. Parameter Contributions:

- Scanning area ratio was the most influential parameter (39.94%), followed by laser power (34.29%) and pattern type (25.77%).
- The 80% scanning area yielded the highest Sq, while 40% resulted in the lowest, demonstrating a non-linear relationship between scanned area and surface roughness.
- Laser power exhibited a fluctuating effect: increasing power from 40 W to 60 W raised Sq, but a drop occurred at 80 W before rising again at 100 W.

3. Surface Hydrophobicity vs. Friction:

- For maximizing hydrophobicity, circular/diamond patterns, 80% scanning area, and 60 W or 100 W laser power were optimal.
- Conversely, minimizing friction required square/hexagonal patterns, 40% scanning area, and 40 W or 80 W laser power.

4.1 Practical Implications

The findings highlight the potential of fiber laser texturing to tailor ST52 steel surfaces for specific applications—whether for hydrophobic coatings in corrosion-resistant environments or low-friction surfaces in mechanical systems. The Taguchi approach proved effective in reducing the number of experimental trials while ensuring robust optimization.

4.2. Future Work

Further studies could explore additional laser parameters (e.g., pulse frequency, scanning speed) and their interactions. Long-term durability assessments of laser-textured surfaces under real operational conditions would also enhance practical applicability.

REFERENCES

1. Nassiri, N., Abbasi, A., Ardestani, M., & Farnia, A. (2023). Effect of welding mode and filler metal on microstructure and mechanical properties of dissimilar joints of S900MC thermomechanical steel to St52 carbon steel welded by gas tungsten arc welding. *Proceedings of the Institution of Mechanical Engineers, Part E: Journal of Process Mechanical Engineering*, *237*(3), 771-781.
2. Radu, S. M., Vîlceanu, F., Toderas, M., Lihoacă, A., & Dinescu, S. (2024). Determining the Level of Structural and Mechanical Degradation of Steel in the Supporting Structure of Mining Excavation Machinery. *Processes*, *12*(1), 153.
3. Sengupta, P., & Manna, I. (2022). Advanced high-temperature structural materials in petrochemical, metallurgical, power, and aerospace sectors—An overview. *Future landscape of structural materials in India*, 79-131.
4. Wypych, G. (2023). *Handbook of Surface Improvement and Modification*. Elsevier.
5. Lausmaa, J. (2001). Mechanical, thermal, chemical and electrochemical surface treatment of titanium. *Titanium in medicine: material science, surface science, engineering, biological responses and medical applications*, 231-266.
6. Adeoye, A. E., Adeaga, O. A., & Ukoba, K. (2024). Chemical Vapour Deposition (CVD) and Physical Vapour Deposition (PVD) techniques: Advances in thin film solar cells. *Nigerian Journal of Technology*, *43*(3), 479-489.
7. Kanchana, R., Ponnuchamy, M., Kapoor, A., & Sethupathi, P. B. (2024). Coatings in the Automobile Application. *Functional Coatings for Biomedical, Energy, and Environmental Applications*, 343-361.
8. Grilli, M. L., Valerini, D., Slobozeanu, A. E., Postolnyi, B. O., Balos, S., Rizzo, A., & Piticescu, R. R. (2021). Critical raw materials saving by protective coatings under extreme conditions: A review of last trends in alloys and coatings for aerospace engine applications. *Materials*, *14*(7), 1656.
9. Sultana, N., Nishina, Y., & Nizami, M. Z. I. (2024). Surface modifications of medical grade stainless steel. *Coatings*, *14*(3), 248.
10. Yeomans, S. R. (2018). Galvanized steel reinforcement: Recent developments and new opportunities. *Proceedings of the 5th International Federation for Structural Concrete*, 7-11.
11. Seshan, K. (Ed.). (2012). *Handbook of thin film deposition*. William Andrew.
12. Saran, R., Ginjupalli, K., George, S. D., Chidangil, S., & VK, U. (2023). LASER as a tool for surface modification of dental biomaterials: A review. *Heliyon*, *9*(6).
13. Wang, H., Deng, D., Zhai, Z., & Yao, Y. (2024). Laser-processed functional surface structures for multi-functional applications-a review. *Journal of Manufacturing Processes*, *116*, 247-283.
14. Arulvel, S., Jain, A., Kandasamy, J., & Singhal, M. (2023). Laser processing techniques for surface property enhancement: Focus on material advancement. *Surfaces and Interfaces*, *42*, 103293.
15. Van Dam, J. P. B., Abrahami, S. T., Yilmaz, A., Gonzalez-Garcia, Y., Terryn, H., & Mol, J. M. C. (2020). Effect of surface roughness and chemistry on the adhesion and durability of a steel-epoxy adhesive interface. *International Journal of Adhesion and Adhesives*, *96*, 102450.
16. Murari, G., Nahak, B., & Pratap, T. (2025). Hybrid surface modification for improved tribological performance of IC engine components–a review. *Proceedings of the Institution of Mechanical Engineers, Part E: Journal of Process Mechanical Engineering*, *239*(3), 1103-1115.

17. Arabian, J. (2020). *Computer integrated electronics manufacturing and testing*. CRC Press.
18. Shetty, R. (2022). DIFFICULT TO MACHINE MATERIALS. *Industrial Engineering*.
19. Machado, A. R., da Silva, L. R. R., Pimenov, D. Y., de Souza, F. C. R., Kuntoğlu, M., & de Paiva, R. L. (2024). Comprehensive review of advanced methods for improving the parameters of machining steels. *Journal of Manufacturing Processes*, *125*, 111-142.
20. Bharathidasan, T., Kumar, S. V., Bobji, M. S., Chakradhar, R. P. S., & Basu, B. J. (2014). Effect of wettability and surface roughness on ice-adhesion strength of hydrophilic, hydrophobic and superhydrophobic surfaces. *Applied surface science*, *314*, 241-250.
21. Pan, R., Cai, M., Liu, W., Luo, X., Chen, C., Zhang, H., & Zhong, M. (2019). Extremely high Cassie–Baxter state stability of superhydrophobic surfaces via precisely tunable dual-scale and triple-scale micro–nano structures. *Journal of Materials Chemistry A*, *7*(30), 18050-18062.
22. Du, R., Gao, X., Feng, Q., Zhao, Q., Li, P., Deng, S., ... & Zhang, J. (2016). Microscopic dimensions engineering: stepwise manipulation of the surface wettability on 3D substrates for oil/water separation. *Advanced Materials*, *28*(5), 936-942.
23. Sushil, K., Ramkumar, J., & Chandraprakash, C. (2025). Surface roughness analysis: A comprehensive review of measurement techniques, methodologies, and modeling. *Journal of Micromanufacturing*, 25165984241305225.
24. Bhushan, B. (2000). Surface roughness analysis and measurement techniques. In *Modern tribology handbook, two volume set* (pp. 79-150). CRC press.
25. Razavifar, M., Abdi, A., Nikooee, E., Aghili, O., & Riazi, M. (2025). Quantifying the impact of surface roughness on contact angle dynamics under varying conditions. *Scientific Reports*, *15*(1), 1-18.
26. Banos, R., Manzano-Agugliaro, F., Montoya, F. G., Gil, C., Alcayde, A., & Gómez, J. (2011). Optimization methods applied to renewable and sustainable energy: A review. *Renewable and sustainable energy reviews*, *15*(4), 1753-1766.
27. Tsui, K. L. (1992). An overview of Taguchi method and newly developed statistical methods for robust design. *Iie Transactions*, *24*(5), 44-57.